

Thermal Conductivity of a Nonequilibrium Chemically Reacting Gas

S. W. BODMAN, P. L. T. BRIAN, and T. C. CHANG

Department of Chemical Engineering,
Massachusetts Institute of Technology, Cambridge, Massachusetts

Thermal conductivity measurements were made for the dissociating system $2\text{NO}_2 \rightleftharpoons 2\text{NO} + \text{O}_2$. Experiments were made at temperatures from 548° to 792°K. and pressures from 1 to 30 atm. Under these conditions the chemical reaction is in a nonequilibrium state, and the rate of energy transport is limited by the rates of the forward and reverse reactions. Experimental results agreed very well with a theoretical model based on a linearized reaction rate expression. Using the thermal conductivity results, it was also possible to determine the chemical kinetic constants for the reaction.

The thermal conductivity of a gas mixture can be significantly augmented if the gas mixture undergoes a reversible chemical reaction. When there is a reversible chemical reaction in the gas phase, a temperature gradient can give rise to concentration gradients, since the chemical equilibrium constant varies with the temperature. Thus, in addition to thermal conduction, there is a flux of chemical enthalpy as a result of the counterdiffusion of chemical reactants and products. This flux of chemical enthalpy may enhance considerably the thermal conductivity of the gas mixture, especially if the enthalpy change of the reaction is large. The problem of the thermal conductivity of a chemically reacting gas mixture is related to the broad field of heat transfer in chemically reacting gases, which has been of recent interest because of its importance to the problem of hypersonic flight (23, 30, 32, 35).

If the chemical reaction is infinitely fast as compared with the rates of diffusion, there will be chemical equilibrium throughout the gas phase and the enhancement of the thermal conductivity is maximized. For such a case, the concentration gradients can be related to the temperature gradient by using the van't Hoff relationship; and the rate of energy transfer due to molecular diffusion can be interpreted in terms of the chemical equilibrium constant, the enthalpy change of the reaction, and the diffusion coefficients. Theoretical as well as experimental aspects of the thermal conductivity of a chemically reacting gas mixture in equilibrium have been thoroughly studied (11, 13, 17, 18, 28, 36). Most previous experimental studies have utilized dissociating nitrogen tetroxide, $\text{N}_2\text{O}_4 \rightleftharpoons 2\text{NO}_2$ (17, 16, 36). The half lives of both forward and reverse reactions are of order microseconds at room temperature, and an equilibrium system having a high enthalpy of reaction can be studied under moderate experimental conditions. Other equilibrium systems have been studied less extensively; examples are the polymerization of hydrogen fluoride, $6\text{HF} \rightleftharpoons (\text{HF})_6$ (24), and the dissociation of phosphorous pentachloride, $\text{PCl}_5 \rightleftharpoons \text{PCl}_3 + \text{Cl}_2$ (14). In all instances experiments on equilibrium systems have sustained theoretical models.

In contrast to the equilibrium case, the frozen system results when the chemical reaction is very slow. In this case no appreciable concentration gradients are sustained

and the increase in thermal conductivity as a result of chemical enthalpy flux can be ignored. Frozen systems have been studied by Srivastava, Barua, and Chakraborti (37) and by Dresvyannikov (21). In both studies, the thermal conductivity was affected only to the very slight extent that the gas composition was altered by the chemical reaction.

Intermediate between equilibrium and frozen systems is the case in which the chemical reaction rate is not fast enough to establish chemical equilibrium, but is sufficiently rapid to establish significant concentration gradients. In this instance the thermal conductivity of the reacting gas mixture depends strongly on the chemical reaction rate. Theoretical studies of the effect of finite chemical reaction rate on the thermal conductivity have been reported (7 to 10, 12, 23), but no experimental data are available in the literature. The only published thermal conductivity data which appear to show the effect of chemical kinetics are the thermal conductivity data reported by Coffin (17) for decomposing nitrogen tetroxide. These data show deviation from the equilibrium theory at pressures less than one-third of an atmosphere. However, a lack of knowledge about the kinetics of the dissociation of nitrogen tetroxide prevented a quantitative comparison of theory and experiment (12).

Experimental data have been reported for convective heat transfer to turbulent nitrogen dioxide at temperatures and pressures where significant concentration gradients existed in the boundary layer (10). These results agreed to within 10% with the film theory solutions of Brian, Reid, and Bodman (8, 9).

Heretofore there have been no experimental results published for the thermal conductivity of a gas which reacts reversibly at a finite rate; thus the present work was undertaken to elucidate the effect of finite reaction kinetics on the thermal conductivity of a stagnant gas. Decomposing nitrogen dioxide was chosen as the chemical system because the chemical kinetics has been studied in considerable detail (2, 3, 5, 6, 33), and because the enthalpy change of the reaction is sufficiently large to increase significantly the thermal conductivity of the gas mixture. Moreover these results provide an invaluable comparison with the

less precise measurements which have been made for heat transfer to this same gas in turbulent flow (10).

THEORY

Since previous papers discuss the necessary theoretical background in detail, only a brief review of pertinent references will be provided here. By linearizing an arbitrary reaction rate expression, Brian and Reid (9) predicted the heat transfer rate in a reversibly reacting gas flowing past a solid wall; they utilized a film model and assumed chemical equilibrium in the bulk region of the gas. When these results are applied to a stagnant reacting gas mixture between two parallel plates, the following result is obtained if the walls are noncatalytic:

$$\phi = \frac{\frac{\sqrt{m\eta}}{\tanh \sqrt{m\eta}}}{1 + \frac{1}{\eta} \left[\frac{\sqrt{m\eta}}{\tanh \sqrt{m\eta}} - 1 \right]} \quad (1)$$

The dimensionless quantity η is the ratio of the thermal conductivity of the gas mixture if it were in chemical equilibrium to the conductivity of the gas mixture which would exist in the absence of the chemical reaction (the frozen thermal conductivity). The variable m may be thought as the ratio of the chemical reaction rate to the rate of molecular diffusion in the gas phase. The parameter ϕ is the ratio of the thermal conductivity of the chemically reacting gas mixture to the frozen thermal conductivity of the gas mixture. For a frozen system m is zero and ϕ is equal to unity, while for an equilibrium system, m approaches infinity and ϕ becomes equal to η .

The case of a chemically reacting gas mixture between two concentric cylinders, such as a hot-wire thermal conductivity cell, has been analyzed by Brokaw (12). To implement Brokaw's results for the $2\text{NO}_2 \rightleftharpoons 2\text{NO} + \text{O}_2$ system, one employs the known kinetic expressions for the second-order forward reaction and for the third-order reverse reaction. It is also convenient and accurate to assume that the binary diffusion coefficients for the pairs $\text{NO}-\text{NO}_2$ and O_2-NO_2 are essentially equal (7). With this information, Brokaw's analysis for the case of noncatalytic walls in the absence of thermal accommodation and temperature jump effects can be summarized as

$$\phi = \frac{\eta}{1 + \frac{(\eta - 1)}{\sqrt{m\eta}}} \quad (2)$$

where the definitions of ϕ and η are identical to those in the parallel plate case. The variable m is still a measure of the chemical reaction rate relative to diffusion rates, but it now becomes a function of system geometry:

$$m = \frac{3k_F}{DC} \frac{P^2 y_{\text{NO}_2}^2}{\xi(1-\xi)} \left[\frac{\tau_o \ln \left(\frac{r_o}{r_w} \right)}{\psi} \right]^2 \quad (3)$$

For a frozen system m is equal to $1/\eta$ and ϕ is equal to unity, while for an equilibrium system, m approaches infinity and ϕ is equal to η .

Both Equations (1) and (2) are the results of linearized analyses, and they are restricted to the case of a small temperature driving force in the gas phase. The effect of a large temperature driving force has been studied by Brian and Bodman (8), who obtained numerically the film model solution for heat transfer accompanied by a

reaction analogous to the nitrogen dioxide decomposition reaction. These results showed that the linearized analyses of previous workers were accurate for surprisingly large values of the temperature driving force. Their results were well approximated by Equation (1) when the temperature driving force was less than 40°F . A temperature driving force of 40°F . in the analysis of Brian and Bodman corresponds to a temperature driving force of 80°F . in a stagnant gas between two parallel plates.

PROPERTIES OF THE $2\text{NO}_2 \rightleftharpoons \text{NO} + \text{O}_2$ GAS MIXTURE

In order to analyze properly the present results, accurate estimates must be available for the thermodynamic and transport properties of $\text{NO}_2-\text{NO}-\text{O}_2$ gas mixtures. The chemical equilibrium for the reaction has been studied thoroughly (4, 25), and is well known. Measurements of the thermal conductivity of nitric oxide and oxygen in the temperature range of interest in this present work have been made by Dresvyannikov (22) and by De Haas (20), respectively. The thermal conductivity of nitrogen dioxide was estimated by extrapolating the experimental data of Coffin and O'Neal (17) up to the temperature range of interest in this present work. The thermal conductivity of the gas mixture was estimated by the method suggested by Cheung (16). The binary diffusion coefficients for the $\text{NO}_2-\text{NO}-\text{O}_2$ system have been estimated by Bodman (7) using the method of Hirschfelder, Curtiss, and Bird (27).

Details regarding the estimation of the properties of the $\text{NO}_2-\text{NO}-\text{O}_2$ gas mixture are discussed in references 7 and 15.

EXPERIMENTAL

A hot-wire thermal conductivity cell, shown schematically in Figure 1, was used for the experimental measurements. The cell body was constructed of a $2\frac{1}{4}$ in. O.D. 304 stainless steel cylinder with a straight and uniform bore of 0.391 in. through its center axis. The hot wire was a 0.00983-in. diam. gold wire, which during measurements was used both as a heater and as a resistance thermometer. The use of a gold wire was necessary

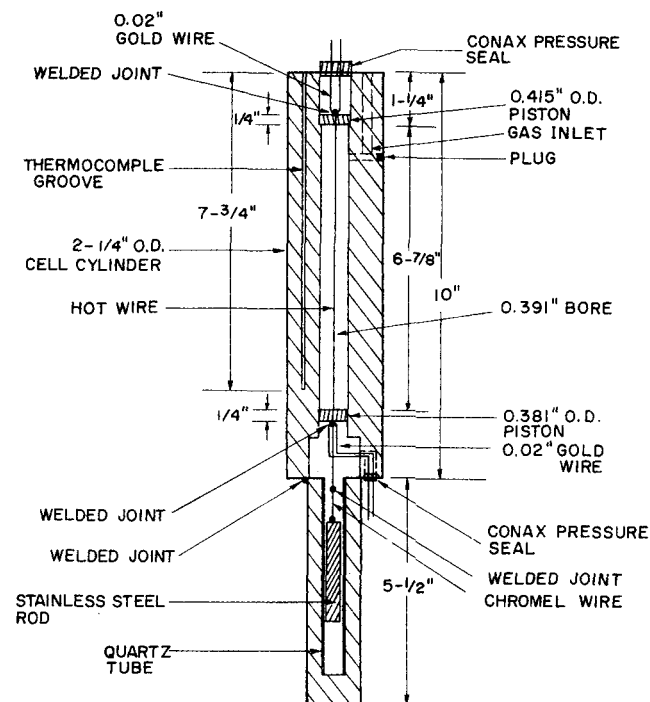


Fig. 1. The hot-wire cell.

because all other commonly used materials, such as platinum, silver, copper, and nickel, react with nitrogen dioxide at high temperatures. Only gold maintained a surface having the required low emissivity value in the presence of NO_2 . The use of stainless steel for the cell body was permitted because the resulting impermeable oxide film prevented further corrosion and because the emissivity of the interior cell wall was not as critical as the wire emissivity in controlling radiative transfer.

The concentricity and straightness of the hot wire were maintained by two centering guides and a stainless steel plumb weight attached to the wire. Two Conax TG type pressure seals were used to seal the two power leads and the two potential leads of the hot wire.

During experimental measurements, a constant current through the hot wire was maintained by a Kepco KS-18-15 constant d.c. power supply. By measuring the current and the voltage drop across the hot wire, the resistance of the hot wire as well as the heat flux was determined. The current through the hot wire was determined by measuring the voltage drop across a 0.1-ohm Leeds and Northrop standard resistor connected in series with the hot wire. The voltage drop was measured with a Rubicon 2780 precision potentiometer. The temperature of the cell wall was measured by a chromel-alumel thermocouple installed in one of the two axial thermocouple grooves provided in the cell wall. The axial temperature profile was determined by moving the thermocouple to various positions in a groove.

To maintain the cell at a constant and uniform temperature, it was put inside a three-zone tubular furnace. Voltage inputs to the three independently controlled heating zones of the furnace were stabilized by a constant voltage regulator.

The piping system, shown in Figure 2, provided for feeding nitrogen tetroxide into the cell. During measurements, nitrogen was in contact with the liquid nitrogen tetroxide. As the pressure in the nitrogen piping was increased, liquid nitrogen tetroxide was forced into the cell.

During experimental measurements, the difference between the temperature of the cell wall and the average temperature of the hot wire ranged from 5° to 25°K . The temperature coefficient of the electrical resistivity of gold needed for computing the gas thermal conductivity was obtained from the experimental data of Dahl (19).

DATA ANALYSIS

The heat fluxes measured in the apparatus of Figure 1 include both radial and nonradial components. For the present cell geometry and thermal conductivities, the effect of nonradial heat flow near the wire ends was analyzed for the case of a nonreacting gas. It was found that including this effect altered the calculated conductivity by only 0.1%, a negligible amount. Thus, in the data analysis, it was assumed that the heat flow in the cell was entirely radial.

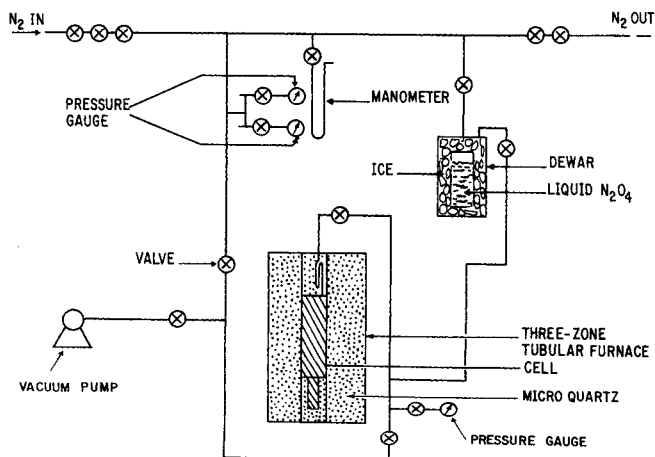


Fig. 2. Piping system for hot-wire cell.

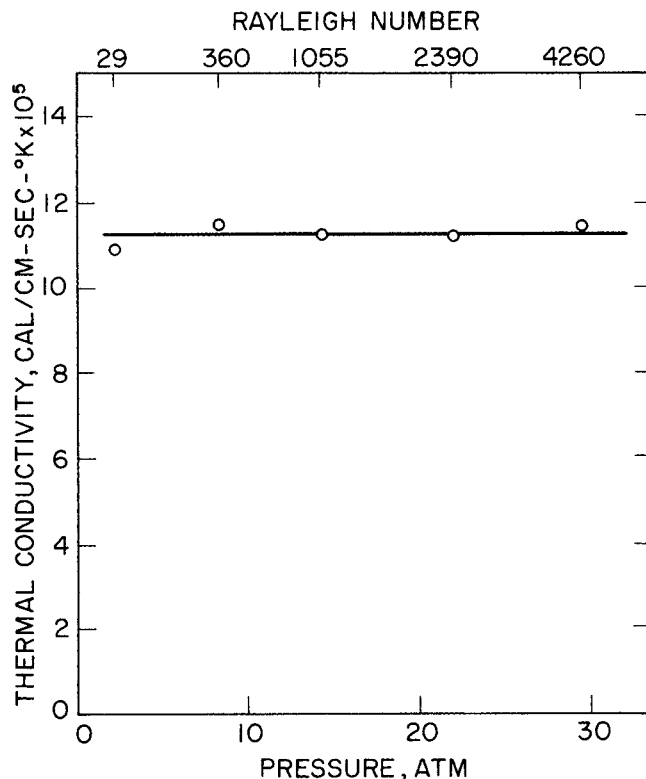


Fig. 3. Results of natural convection runs; nitrogen gas.

In computing the thermal conductivity for each experiment, corrections were made for the radiative loss from the hot wire. Both the radiative loss from the hot wire to the cell wall and the radiative loss from the hot wire to the dissociating nitrogen dioxide gas mixture were accounted for. The emissivity of the hot wire was determined by comparing the apparent thermal conductivity of nitrogen obtained in this work with the thermal conductivity of nitrogen determined by Rothman (34). The absorptivities of nitrogen dioxide and nitric oxide used in calculating radiation to the gas were obtained from references 26, 29, and 31. The results indicated an emissivity value of 0.06 for the gold. The emissivity reached this value after the first few exposures to nitrogen dioxide, and it remained stable during the entire experimental program. The maximum radiation contribution required a 6% correction to the measured conductivity value. Details of the corrections employed are reported elsewhere (15).

RESULTS AND DISCUSSION

Natural Convection

The possibility of natural convection effects in the cell was investigated by carrying out a series of nitrogen runs at 617°K . and at pressures of 2.42 to 29.4 atm. The results of these runs are summarized in Figure 3, which shows the thermal conductivity of nitrogen as a function of pressure. The variation in the nitrogen density caused a 146-fold change in Rayleigh number from 29 to 4,260. The figure shows that this variation in Rayleigh number causes no change in the measured conductivity.

In reacting gas systems, the density gradient is caused not only by the temperature gradient but also by the concentration gradient in the system. These effects tend to reinforce one another. For the present system a conservative value of the Rayleigh number was computed by assuming chemical equilibrium and employing the density change due to both temperature and composition effects.

The maximum Rayleigh number computed in this fashion for all nitrogen dioxide experiments was 11,000; thus it was concluded that free convection effects were not significant in any of the present work.

Frozen Systems

In order to interpret meaningfully the experimental results for reacting cases, the thermal conductivity of frozen mixtures of $\text{NO}_2\text{-NO-O}_2$ must be known accurately. A number of runs were made with dissociating nitrogen dioxide at frozen conditions by lowering the system pressure and thus the chemical reaction rate. All results having a theoretical value of $\phi \leq 1.03$ were considered to be frozen. Since only a small correction was required, the frozen thermal conductivity value could be determined by taking the ratio $k_{\text{exp}}/\phi_{\text{theo}}$.

To achieve frozen conditions, subatmospheric pressures were required. Initial results reflected a dependence on pressure which suggested that thermal accommodation and temperature jump effects were important at low pressure. For cases when these effects are in evidence, Archer (1) has developed the following relation:

$$K' = K - \frac{15}{2\pi} \left(\frac{2 - \alpha}{\alpha} \right) \frac{P_0}{P} \frac{K}{\ln \left(\frac{r_0}{r_w} \right)} \frac{\lambda}{r_w} \quad (4)$$

where K' is the apparent thermal conductivity and the second term on the right-hand side accounts for the effects of temperature jump and incomplete energy exchange between the hot wire and gas. In accordance with this

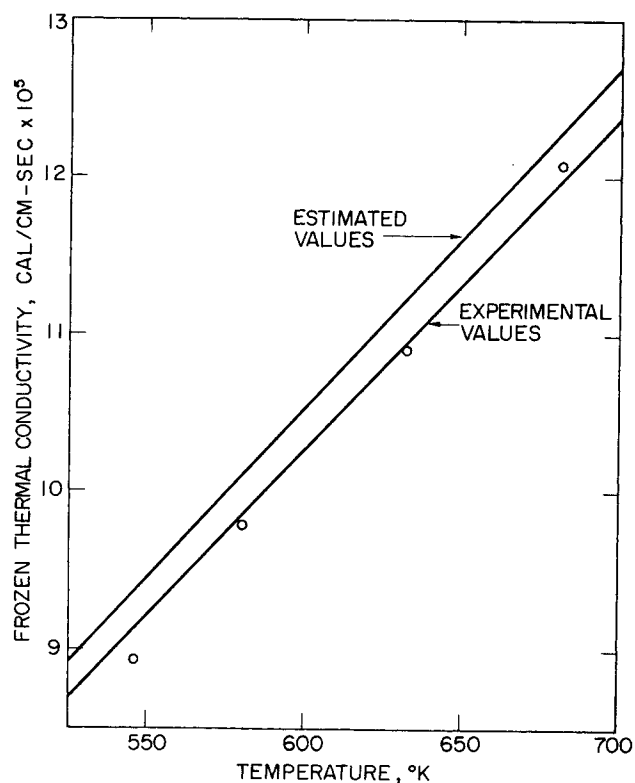


Fig. 5. Frozen thermal conductivity. A comparison of experimental results with theoretical prediction.

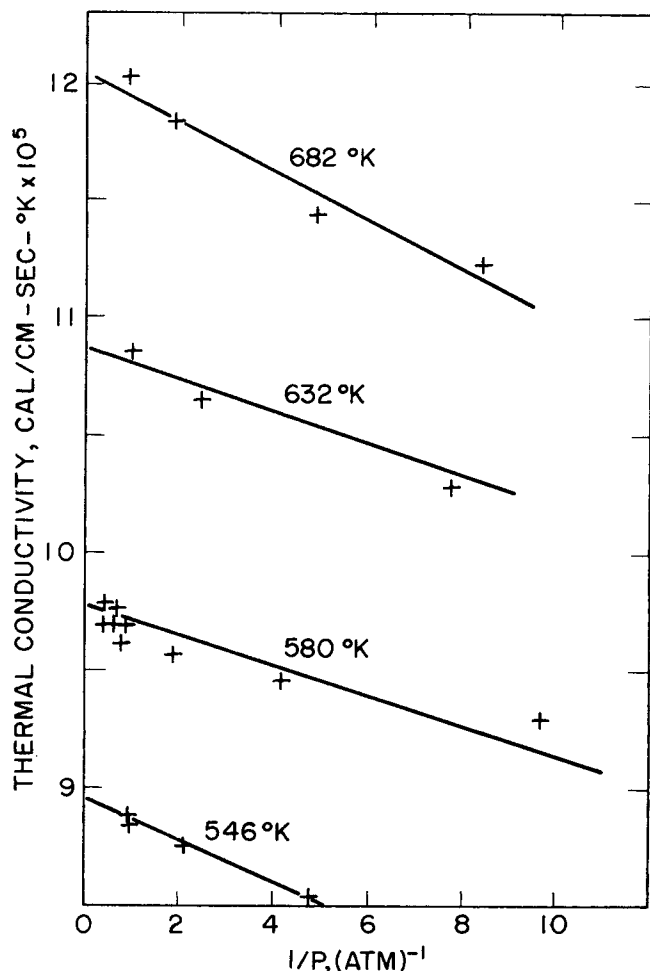


Fig. 4. Results of frozen runs.

equation, Figure 4 shows isothermal frozen conductivities plotted versus the reciprocal of pressure. In interpreting this figure, it should be remembered that the composition of the gas varies along each isotherm due to the influence of pressure on chemical equilibrium. This effect tends to distort the linearity predicted by Equation (4). Nevertheless, the effect of chemical composition is significantly less than the variation seen in Figure 4, and it is concluded that accommodation effects are indeed influencing the experimentally observed frozen conductivities.

As seen in Figure 4, the effects of accommodation were substantially eliminated only at pressures above 1 atm. However, frozen conditions could be achieved in this temperature range only at pressures below approximately 2 atm. Thus the most accurate data for frozen conductivity were measured for each temperature at pressures between 1 and 2 atm. Figure 5 shows a comparison of these data with values computed from pure component data on NO_2 , NO , and O_2 (17, 20, 22) and the mixing rule of Cheung (16). It is seen that there is a consistent negative 2.5% deviation of experiment from theory. When compared with the theoretical predictions of Svehla and Brokaw (38), the experimental data deviated negatively approximately 1% from theory. The consistency of the departure of experiment from theory, in spite of wide variations in system composition ($0.25 < y_{\text{NO}_2} < 0.85$), probably results from slight imperfections in the mixing rules as applied to this system. The subsequent data on reacting gases were compared with frozen conductivity values computed using pure component data, Cheung's mixing rule, and a constant 2.5% negative correction.

Effect of Chemical Reaction

The thermal conductivity of dissociating nitrogen dioxide was measured over a pressure range of 1 to 30 atm. and at temperatures from 548° to 792°K. Figure 6 presents some examples of the results obtained, with the equilibrium

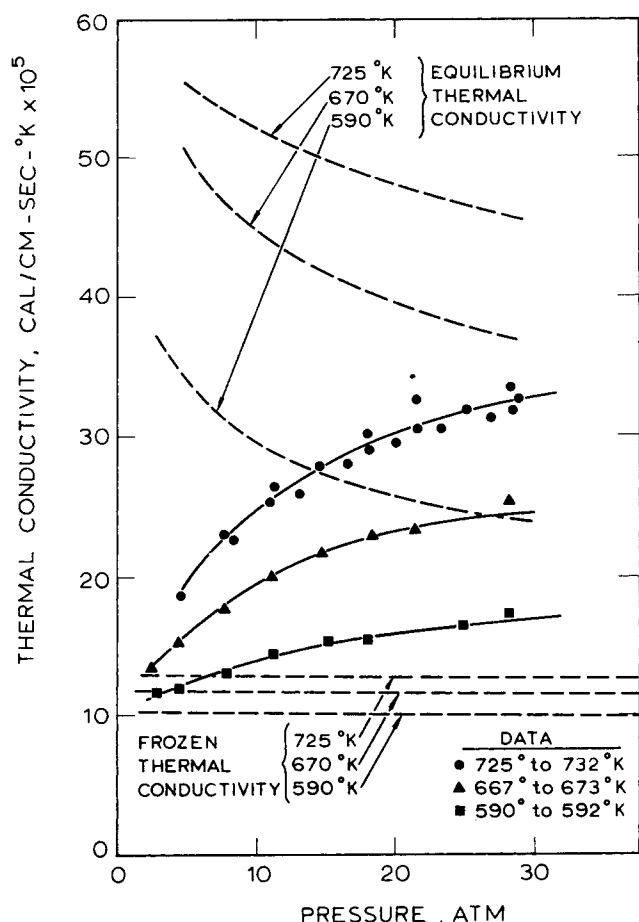


Fig. 6. Thermal conductivity of reacting mixture.

and the frozen thermal conductivities shown for comparison. In marked contrast to the results in the frozen regime, the data in the higher regions of temperature and pressure showed a marked dependence on temperature and pressure. Experimental ϕ values were computed by taking the ratio of the experimental thermal conductivity to the frozen conductivity computed at the pressure and average temperature in the cell. Values of m and η were also computed at the average temperature; these calculations utilized $\text{NO}_2\text{-NO}$ and $\text{NO}_2\text{-O}_2$ diffusion coefficients as estimated by Hirschfelder's method (27) and chemical kinetic data as reported by Rosser and Wise (33).

Equation (2) was used as a theoretical basis for evaluating the data for the reacting gas runs. This linearized result could be used directly because the maximum temperature driving force of the present work was 25°C ., a value well below the 45°C . limit for accuracy of a linear model (8). An approximate but graphic means of comparing experiment and theory is shown in Figure 7, where ϕ is plotted versus \sqrt{m} for parametric values of η . In order to avoid crowding, this figure includes only a portion of the experimental data. Since each experimental point corresponds to a different value of η , the data have been bracketed into ranges of η and are compared with a theoretical line corresponding to the midpoint of the range. This figure reveals an excellent corroboration of the theoretical model and demonstrates the utility of m and η in describing the effects of a reversible reaction on thermal conductivity.

A quantitative comparison of theory and experiment is presented in Figure 8, which shows for each run the experimental ϕ value plotted versus that predicted by Equation (2). The maximum departure of experiment from

theory is approximately 10% and the average deviation is about 3%; the deviations are approximately normally distributed about the mean. An average deviation of 3% compares very favorably with the most probable values of the experimental precision which were estimated in an analysis of experimental errors.

Another way to compare experiment and theory is to use Equation (2) to compute the reaction rate constant from the experimental thermal conductivity data. Thus the right-hand side of Equation (2) is set equal to the experimental ϕ value, and the resulting equation is solved for m . From this m value, the reaction rate constant k_F can be determined from Equation (3). The Arrhenius plot of the reaction rate constant thus determined is shown in Figure 9. Some of the data points have been omitted in the figure to avoid crowding. The solid line in the figure represents the best line for the data of Rosser and Wise. It is seen that the reaction rate constant determined from the thermal conductivity measurements agrees very well with the data

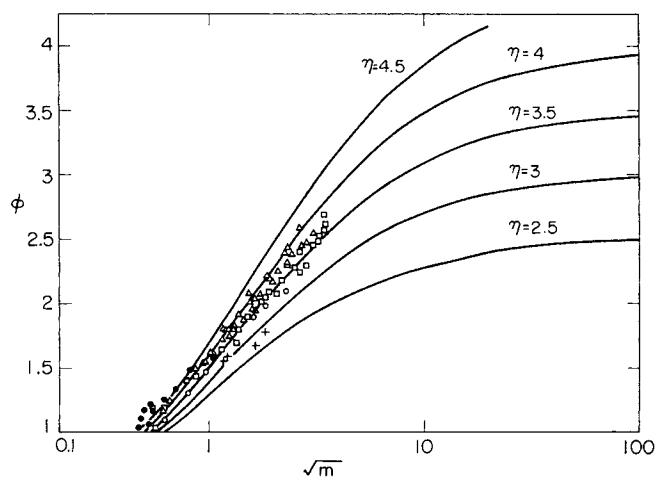


Fig. 7. Correlation of data on thermal conductivity in the presence of a reversible chemical reaction. + $2.44 \leq \eta \leq 2.75$. \circ $2.75 \leq \eta \leq 3.25$. \square $3.25 \leq \eta \leq 3.75$. \triangle $3.75 \leq \eta \leq 4.25$. \bullet $4.25 \leq \eta \leq 4.89$.

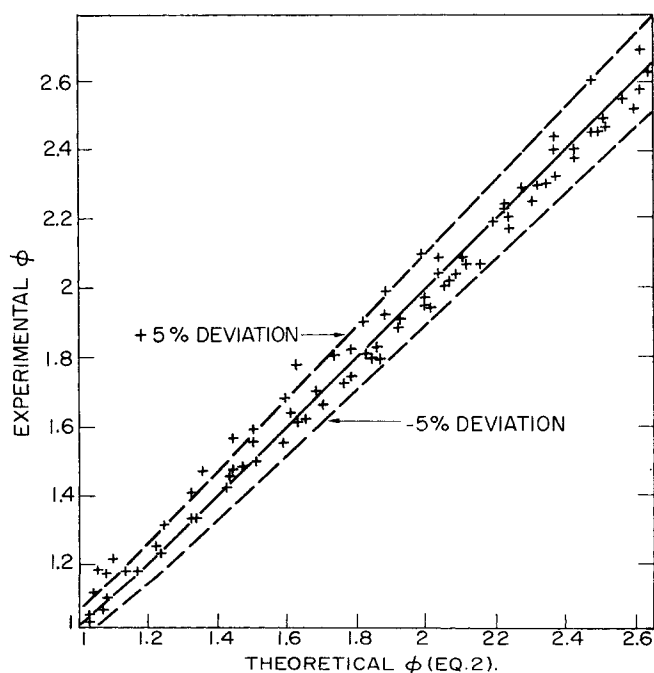


Fig. 8. Comparison of experimental and theoretical values of ϕ .

of Rosser and Wise. The agreement between the experimental and the literature values of the chemical reaction rate constant over a wide range of temperature provides another strong confirmation of the experimental results of this work and of the theory previously developed. It also suggests that measurements of thermal conductivity may provide a valuable means of estimating chemical kinetic parameters for reversible reactions having half-lives in the millisecond range.

The percentage scatter of the reaction rate constant determined from the thermal conductivity measurements as shown in Figure 9 is much greater than the scatter of the experimental ϕ values from the theoretical ϕ values as shown in Figure 8. This is because at low temperature ϕ is a relatively insensitive function of the chemical reaction rate. This can be seen in Figure 10, which shows the sensitivity of ϕ with respect to the chemical reaction rate under typical experimental conditions. Figure 10 shows that even in the region of maximum sensitivity, a 100% change in the reaction rate results in a change of only about 11% in ϕ .

Figure 10 also shows that the sensitivity of ϕ with respect to the chemical reaction rate is highest when the ϕ value is in the range of approximately 1.1 to 2.5. For most of the nitrogen dioxide runs the experimental ϕ values lie in this range. Thus most of the nitrogen dioxide runs were carried out under conditions for which the theory of a nonequilibrium, chemically reacting gas mixture can best be tested.

As already mentioned, the diffusion coefficient values exert a strong influence on the calculation of ϕ ; the values used in the present data analysis were those estimated previously (7) using Hirschfelder's method (27). Since there are no experimental data available for the binary diffusion coefficients for any combination of NO_2 , NO , and

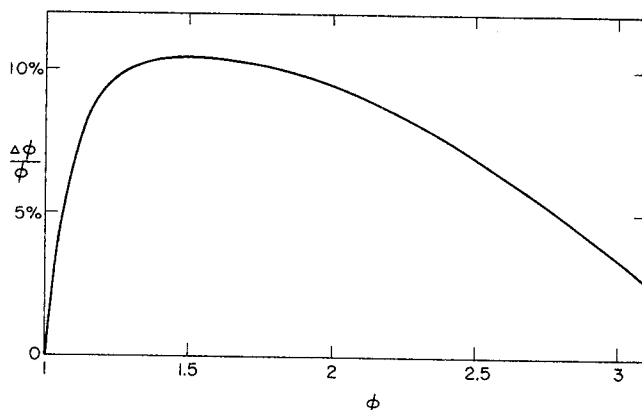


Fig. 10. Sensitivity of ϕ to the chemical reaction rate. $T = 750^\circ\text{K}$; $P = 10 \text{ atm.}$; $\eta = 3.41$; $\Delta\phi$ = increase in value of ϕ when reaction rate constant is doubled.

O_2 , there is uncertainty regarding the accuracy of the estimated diffusion coefficients. The close agreement between experiment and theory in this work, as well as that in the work of Brian, Reid, and Bodman (10), lends support to the accuracy of Hirschfelder's method for the present system.

The analyses of the present experimental results assumed that the dissociation of nitrogen dioxide was a homogeneous reaction, and that neither gold nor stainless steel catalyzed the reaction. Previous work (7, 10) has indicated a lack of catalytic activity of these metals; the close agreement of theory and experiment in the present study lends further substance to this assertion.

CONCLUSIONS

Measurements of the thermal conductivity of dissociating nitrogen dioxide have been made over a wide range of temperature and pressure. Under these experimental conditions, the gas mixture was not in chemical equilibrium, but the thermal conductivity was significantly augmented by the chemical reaction. The effect of chemical kinetics on the thermal conductivity was clearly demonstrated.

The experimental results are presented in terms of the parameter ϕ , which is the factor by which the chemical reaction enhances the thermal conductivity. The experimental results were found to agree well with the linearized analysis of Brokaw, generalized by Brian and Reid. The average deviation of experiment from theory was 3%. This deviation agreed well with the probable precision estimated in an analysis of experimental errors.

The chemical reaction rate constant as well as the activation energy for the decomposition of nitrogen dioxide determined from the thermal conductivity measurements agrees well with chemical kinetic data reported in the literature. This not only provides further confirmation of both the experimental results and the theory, but also illustrates the utility of thermal conductivity measurements in obtaining chemical kinetic data for a nonequilibrium, chemically reacting gas mixture.

ACKNOWLEDGMENT

The authors gratefully acknowledge Socony Mobil Oil Company, Rohm and Haas Company, and the MIT Center for Space Research, which provided financial support for portions of this work. Computations were carried out at the MIT Computation Center. T. C. Chang was supported by an Arthur D. Little Fellowship.

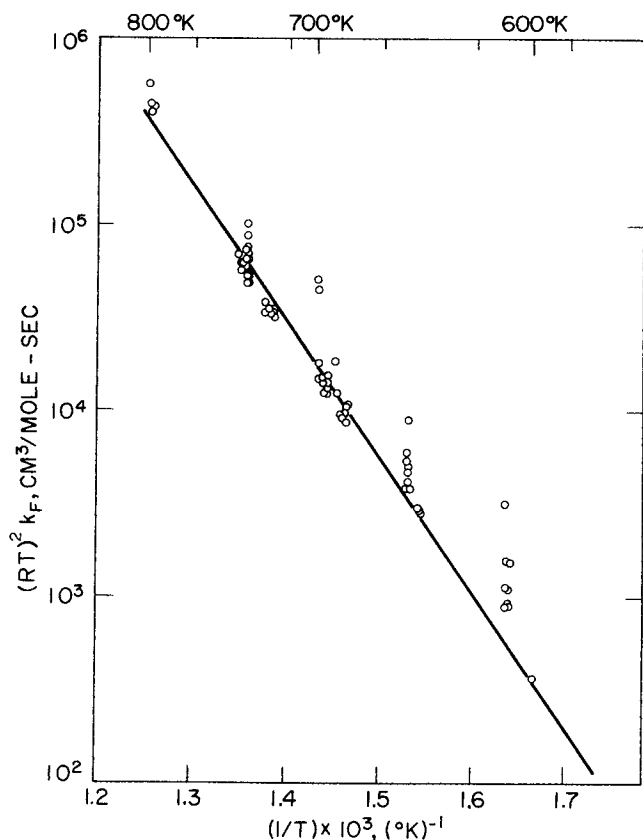


Fig. 9. Chemical kinetic constant for the decomposition of nitrogen dioxide as determined by thermal conductivity measurements.

NOTATION

- C = total molar concentration, moles/cu. cm.
 D = binary diffusion coefficient for NO-NO₂ or O₂-NO₂, sq. cm./sec.
 D_{ij} = binary diffusion coefficient of component i in component j , sq. cm./sec.
 \mathcal{D}_k = effective diffusivity of component k in a multi-component mixture, defined by

$$\frac{1}{\mathcal{D}_k} = \sum_{j \neq k} \frac{y_j - \left(\frac{\omega_j}{\omega_k}\right) y_k}{D_{jk}}$$

- f = function relating homogeneous rate for the reaction $a_1 A_1 + a_2 A_2 + a_3 A_3 + \dots \rightleftharpoons b_1 B_1 + b_2 B_2 + b_3 B_3 + \dots$, moles/(sec.) (cu.cm.)
 f_T = $(\partial f / \partial T) y_{A_1}, y_{A_2}, y_{A_3} \dots y_{B_1}, y_{B_2}, y_{B_3} \dots$, moles/(sec.) (cu.cm.) (°K.)
 f_{A_1} = $(\partial f / \partial y_{A_1})_T$, all y 's except y_{A_1} . Similar definition for $f_{A_2}, f_{B_1}, f_{B_2} \dots$, moles/(sec.) (cu.cm.)
 f_y = $f_{A_1} = \sum_{i \neq 1} f_{A_i} S_{A_i A_1} + \sum_{\text{all } j} f_{B_j} S_{B_j A_1}$, moles/(sec.) (cu.cm.)
 ΔH = enthalpy change of reaction, cal./g.-mole and cal./mole of nitrogen dioxide in this experimental work
 I_0 = hyperbolic Bessel function
 I_1 = hyperbolic Bessel function
 K_0 = hyperbolic Bessel function
 K_1 = hyperbolic Bessel function
 K = thermal conductivity, cal./(sec.) (cm.) (°K.)
 K' = apparent value of K
 K_f = thermal conductivity of gas mixture in frozen condition, cal./(sec.) (cm.) (°K.)
 k_F = kinetic constant for the decomposition of nitrogen dioxide, mole/(sec.) (cc.) (atm.²)
 L = half length of the hot wire, cm.

$$m = \frac{3k_F P^2 y_{\text{NO}_2}^2}{D C \xi (1 - \xi)} \left[\frac{r_o \ln \left(\frac{r_o}{r_w} \right)}{\Psi} \right]^2 \quad \text{for the hot-wire cell}$$

- m = $f_y x_F^2 / C D_A$ for gas between parallel plates
 P = pressure, atm.
 P_{NO_2} = partial pressure of nitrogen dioxide, atm.
 r_o = inside radius of the outside cylinder, cm.
 r_w = radius of hot wire, cm.
 S_{ij} = $(D_j / D_i) (\omega_i / \omega_j)$
 T = temperature, °K.
 x_F = half of the gap width between two parallel plates, cm.

- y_{NO_2} = mole fraction for nitrogen dioxide
 z = axial distance, cm.

$$Z = \pi z / 2L$$

$$Z_1 = \chi r_w$$

$$Z_2 = \chi r_o$$

Greek Letters

- α = thermal accommodation coefficient
 η = $1 + \frac{f_T \Delta H C D_A}{f_y K_f}$, in general, and $1 + \left(\frac{\Delta H^2}{RT^2} \right) \left(\frac{DC}{K_f} \right) \frac{\xi(1 - \xi)}{6}$ for this chemical system
 λ = mean free path of gas molecules, cm.
 ξ = degree of advancement for the decomposition reaction
 ϕ = K / K_f
 χ = $\left[\frac{3\eta k_F}{DC} \frac{P^2 y_{\text{NO}_2}^2}{\xi(1 - \xi)} \right]^{1/2}$

$$\omega_j = \text{stoichiometric coefficient for component } j; \text{ positive for reactants and negative for products}$$

$$\Psi = \frac{(r_o/r_w) I_0(Z_2) - I_1(Z_1)}{K_1(Z_2) I_1(Z_1) - K_1(Z_1) I_1(Z_2)} \times [K_0(Z_2) - K_0(Z_1)] + \frac{(r_o/r_w) K_1(Z_2) - K_1(Z_1)}{I_1(Z_1) K_1(Z_2) - I_1(Z_2) K_1(Z_1)} \times [I_0(Z_2) - I_0(Z_1)]$$

LITERATURE CITED

1. Archer, C. T., *Phil. Mag.*, **19**, 901 (1935).
2. Ashmore, P. G., and M. G. Burnett, *Trans. Faraday Soc.*, **58**, 253 (1962).
3. ———, and B. J. Tyler, *ibid.*, 685.
4. Bodenstein, M., et al., *Z. Phys. Chem.*, **100**, 82 (1922).
5. *Ibid.*, 106.
6. Bodenstein, M., and L. Wachenheim, *Z. Electrochem.*, **24**, 183 (1918).
7. Bodman, S. W., Sc.D. thesis, Massachusetts Inst. Technol., Cambridge (1964).
8. Brian, P. L. T., and S. W. Bodman, *Ind. Eng. Chem. Fundamentals*, **3**, 339 (1964).
9. Brian, P. L. T., and R. C. Reid, *AIChE J.*, **8**, 322 (1962).
10. ———, and S. W. Bodman, *ibid.*, **11**, 809 (1965).
11. Brokaw, R. S., *J. Chem. Phys.*, **32**, 1005 (1960).
12. *Ibid.*, **35**, 1569 (1961).
13. Butler, J. N., and R. S. Brokaw, *ibid.*, **26**, 1636 (1957).
14. Chakraborti, P. K., *ibid.*, **38**, 575 (1963).
15. Chang, T. C., Sc.D. thesis, Massachusetts Inst. Technol., Cambridge (1968).
16. Cheung, H., *Univ. California UCRL-8230* (1958).
17. Coffin, K. P., *J. Chem. Phys.*, **31**, 1290 (1959).
18. ———, and C. O'Neal, *NACA TN 4209* (1958).
19. Dahl, A. I., in "Gold; Recovery, Properties, and Applications," p. 70, E. M. Wise, D. Van Nostrand, New York (1964).
20. De Haas, and A. A. Westenberg, *Phys. Fluids*, **6**, 617 (1963).
21. Dresvyannikov, F. N., and G. A. Mukhachev, *Mater. Konf. Molodykh. Nauch. Robot. Kazan., Sekts. Fiz.-Tekh. Mekhan.-Mat.*, 2nd., Kazan (1965).
22. Dresvyannikov, F. N., *Teploenergetika*, **13**, 86 (1966).
23. Fay, J. A., and F. R. Riddell, *J. Aeronaut. Sci.*, **25**, 73 (1958).
24. Franck, E. U., and W. Spalthoff, *Naturwissenschaften*, **40**, 580 (1953).
25. Giaque, W. F., and J. D. Kemp, *J. Chem. Phys.*, **6**, 40 (1938).
26. Guttman, A., *J. Quant. Spectr. & Radiative Transfer*, **2**, 1 (1962).
27. Hirschfelder, J. O., C. F. Curtiss, and R. B. Bird, "Molecular Theory of Gases and Liquids," Wiley, New York (1954).
28. Hirschfelder, J. O., *J. Chem. Phys.*, **26**, 274 (1957).
29. Hottel, H. C., and A. F. Sarofim, "Radiative Transfer," McGraw-Hill, New York (1967).
30. Leeds, L., *Jet Propulsion*, **26**, 259 (1956).
31. Malkmus, W., and A. Thompson, *J. Quant. Spectr. & Radiative Transfer*, **2**, 16 (1962).
32. Rose, P. H., and W. I. Stark, *J. Aeronaut. Sci.*, **25**, 86 (1958).
33. Rosser, W. A., and H. Wise, *J. Chem. Phys.*, **24**, 493 (1956).
34. Rothman, A. J., and L. A. Bromley, *Ind. Eng. Chem.*, **47**, 899 (1955).
35. Sclar, S. M., *J. Aeronaut. Sci.*, **25**, 273 (1958).
36. Srivastava, B. N., and A. K. Barua, *J. Chem. Phys.*, **35**, 329 (1961).
37. ———, and P. K. Chakraborti, *Trans. Faraday Soc.*, **59**, 2522 (1963).
38. Svehla, R. A., and R. S. Brokaw, *NASA TN D-3327* (1966); see also *J. Chem. Phys.*, **44**, 4643 (1966).

Manuscript received January 6, 1971; revision received March 19, 1971; paper accepted March 22, 1971.